BIOCHEMISTRY
including biophysical chemistry & molecular biology
Article

Biochemistry **2009,** *48,* 12089–12095 12089
DOI: 10.1021/bi901380c

Effect of Chloride Binding on the Thermal Trimer−Monomer Conversion of Halorhodopsin in the Solubilized System[†]

Takanori Sasaki,[‡,§] Tomoyasu Aizawa,[‡] Masakatsu Kamiya,[‡] Takashi Kikukawa,[∥] Keiichi Kawano,[∥] Naoki Kamo,[⊥] and Makoto Demura*[,‡]

[‡]*Faculty of Life Science, Hokkaido University, Sapporo 060-0810, Japan,* [§]*School of Science and Technology, Meiji University, Tama-ku, Kawasaki-shi, Kanagawa 214-8571, Japan,* [∥]*Graduate School of Science, Hokkaido University, Sapporo 060-0810, Japan, and* [⊥]*College of Pharmaceutical Sciences, Matsuyama University, Bunkyo-cho, Matsuyama 790-8578, Japan*

Received August 8, 2009; Revised Manuscript Received November 18, 2009

ABSTRACT: Halorhodopsin from *Natronomonas pharaonis* (NpHR) acts an inward-directed, light-driven chloride pump and forms a homotrimer. To evaluate effect of trimeric assembly, that is, intermolecular interaction, on the control or modulation of light-driven chloride pumping activity of individual HRs, it is important to understand the thermal and chloride sensitivity of trimer dissociation and the structural stability of HR. In this study, the thermal dissociation of NpHR trimer to monomer in a dodecyl β-D-maltoside-solubilized system was investigated, using size-exclusion chromatography and visible absorption. In the absence of Cl^-, NpHR retained the trimer assembly at 25 °C but dissociated to the monomer with an increase in temperature to > 40 °C. On the other hand, in the presence of Cl^-, the trimer assembly was maintained at 40 °C. The dissociation of the trimer to the monomer after incubation at 40 °C, which was determined via size-exclusion chromatography, depended on the Cl^- concentration and showed a sigmoidal isotherm. From this isotherm, the apparent dissociation constant for Cl^- was estimated to be 22 mM with a Hill coefficient of 2.2. A similar isotherm was obtained when SO_4^{2-} was used instead of Cl^- with a dissociation constant of 94 mM. On the other hand, thermal dissociation of the NpHR trimer to the monomer in the absence of Cl^- proceeded by two components: the fast component is susceptible to the changes in temperature and detergent concentration, and the slow component is accompanied by bleaching at the same time. Activation energies of the fast and slow dissociation components and bleaching were 57.8, 35.3, and 40.5 kcal/mol, respectively. The presence of a second chloride-binding site with a Hill coefficient of ∼2 at the surface of NpHR to control the trimer−monomer conversion was discussed.

Halorhodopsin (HR) is a transmembrane, seven-helix retinal protein in the membrane of the archaeal bacterium that acts as an inward-directed, light-driven chloride ion pump (*1*−*5*). Since the primary structures of HR from *Halobacterium salinarum* (HsHR) and *Natronomonas pharaonis* (NpHR)[1] are very highly homologous (55%), their tertiary structures would be conserved. One of the greatest advantages of NpHR compared to HsHR is its stability, especially in a chloride-free system, and NpHR obtained from a recently reported *Escherichia coli* expression system (*6*−*8*) can be solubilized with a mild nonionic detergent without being denatured.

To clear the light-driven chloride ion pump mechanism of HR, the roles played by putative anion-binding sites in the cytoplasmic and extracellular channels of NpHR have been investigated using the wild-type and various mutant proteins in the solubilized system, all of which were functionally expressed in *E. coli* cells (*9*−*15*). NpHR binds a retinal chromophore to Lys-256 in the seventh helix G through a Schiff base linkage and has a Cl^- binding site in the vicinity of the retinal Schiff base (*16*) with a dissociation constant (K_d) of 1−5 mM (*3*, *9*, *17*). Moreover, another weaker predicted Cl^- binding site on the extracellular (EC) side has been proposed (*4*, *18*−*20*). However, the relationship between the weaker Cl^- binding site and the Cl^- channel structure is unknown.

Two-dimensional crystals of HR from *H. salinarum* (HsHR) have been obtained using overexpressing *H. salinarum* strain D2 (*16*). Atomic force microscopy (AFM) (*21*) and electron cryomicroscopy (*22*) have revealed that the crystal form of the isolated HsHR consists of one membrane in which alternating tetramers are oriented in opposite directions. In these reports, it was not known whether this orientation occurs by misinsertion of some of the molecules in vivo or by adventitious fusion at some point during isolation. In contrast, X-ray diffraction of HsHR crystallized in a lipidic phase showed the trimeric form (*16*). Therefore, from these reports, it is suggested that the oligomeric states of HsHR are influenced by the reconstituting condition.

Recently, we have reported that the solubilized NpHR, which was functionally expressed in *E. coli* cells, forms the trimer structure even in the presence of 0.1 (2 mM) to 1% (20 mM) dodecyl β-D-maltoside (DDM) (*23*). This conclusion was drawn from the following observations: exciton coupling of visible circular dichroism (CD) spectrs (*24*−*28*), size-exclusion chromatography, and sodium dodecyl sulfate−polyacrylamide gel electrophoresis (SDS−PAGE) and mass spectra of the cross-linked

[†]This study was partially supported by Grants-in-Aid for Scientific Research in Priority Areas from and the National Project on Targeted Protein Research Program of the Ministry of Education, Culture, Sports, Science and Technology of Japan.

*To whom correspondence should be addressed: Faculty of Advanced Life Science, Hokkaido University, Sapporo 060-0810, Japan. E-mail: demura@sci.hokudai.ac.jp. Phone and fax: +81-11-706-2771.

[1]Abbreviations: NpHR, *pharaonis* halorhodopsin; BR, bacteriorhodopsin; DDM, dodecyl β-D-maltoside.

© 2009 American Chemical Society
Published on Web 11/18/2009

NpHR by glutaraldehyde. Using the membrane fractions expressing NpHR (*E. coli* and *H. salinarum*), visible CD spectra showed exciton coupling, which suggests strongly the trimer structure in the cell membrane. Moreover, NpHR functionally expressed in *Xenopus laevis* oocytes, nerve cells, and *Caenorhabditis elegans* allows photocurrents by illumination (*29*, *30*), suggesting unidirectional orientation of the NpHR trimer. In addition, in the previous report (*23*), it was found that the trimer association is influenced by temperature and chloride concentration; that is, the NpHR monomer is prepared by being moderately heated at 40 °C and chilled in the absence of Cl^-. When the rate of photobleaching of trimeric NpHR by hydroxylamine was measured at room temperature, only 2% of the NpHR were marginally bleached in the presence of 300 mM NaCl under continuous illumination for 30 min. In the case of monomeric NpHR in the presence of Cl, the photobleaching rate was remarkably high (52% of NpHR was bleached by the illumination). However, details of the chloride dependency of the NpHR trimer in the DDM-solubilized system were unknown. To evaluate the effect of trimeric assembly, that is, intermolecular interaction, on the control or modulation of the light-driven chloride pumping activity of individual HRs, it is important to understand the thermal and chloride sensitivity of trimer dissociation and the structural stability of HR.

In this study, thermally induced dissociation and bleaching processes of the NpHR trimer in the DDM micelle system were investigated systematically using size-exclusion chromatography and visual absorption spectroscopy. These experiments revealed that the thermal dissociation of the NpHR trimer at 40 °C scarcely occurred in the presence of Cl^-, because of the specific anion binding to the protein. On the other hand, in the absence of Cl^-, thermal dissociation of the NpHR trimer to the monomer occurred by two kinetic components. The dissociation mechanism of the trimeric structure depending on the secondary Cl binding site and the bleaching of NpHR in the absence of anions are discussed.

MATERIALS AND METHODS

Expression and Purification of Trimeric NpHR. Expression of the histidine-tagged protein and purification procedures using *E. coli* BL21(DE3) cells harboring the plasmid were performed by the methods of Sato et al. (*8*). The expressed NpHR on the *E. coli* membrane was extracted by the solubilization of 1.5% DDM (Dojindo Lab, Kumamoto, Japan), and a fraction of the solubilized sample was collected by using Ni-NTA agarose (Qiagen, Hilden, Germany) with 50 mM Tris-HCl (pH 7.0), 300 mM NaCl, 150 mM imidazole, and 0.1% DDM. The NpHR solution was desalted once by being passed over a PD-10 column (Amersham Biosciences, Uppsala, Sweden) in 10 mM Mops buffer (pH 7.0) containing 0.1% DDM to adjust the NaCl concentration. After this buffer exchange, the protein concentration was estimated using an extinction coefficient ε_{600} of 50000 M^{-1} cm^{-1} (*17*).

The number of NpHR molecules as an oligomer unit in a DDM micelle was identified using gel filtration chromatography, mass spectrometry, and SDS−PAGE, as described in a previous report (*23*). Briefly, the samples were applied to a Superdex 200 10/300 GL size-exclusion column (Amersham Biosciences) previously equilibrated with 50 mM NaP_i (pH 7.0), 150 mM NaCl, and 0.1% DDM. The column was run at a flow rate of 500 μL/min and an available pressure of 80 psi, and eluting proteins were simultaneously monitored at 280 nm. The gel filtration peaks of the DDM−NpHR complex observed at 1350 and 1500 s were assessed to be ~265 and ~136 kDa (M_w) based on the standard calibration curve, respectively. The former and latter M_w values agreed with the sum of three NpHR molecules and the DDM molecules which were closely packed over the entire hydrophobic surface area of the HR trimer and the sum of one NpHR molecule and the surrounding DDM molecules, respectively. Using the chemical cross-linking of NpHR with 1% glutaraldehyde, the presence of trimeric and monomeric NpHRs in the DDM detergent was confirmed by SDS−PAGE and mass spectrometry by employing the two-layer method (*31*).

Measurement of Trimer Dissociation and Absorption Spectroscopy. DDM−NpHR samples (20 μM) once desalted by being passed over Sephadex-G 25 in a PD-10 column (8.3 mL; Amersham Pharmacia Biotech, Uppsala, Sweden) were incubated in the presence or absence of NaCl for 3 h at 40 °C. Then, each sample was rapidly cooled in ice and water to quench the dissociation step, followed by application to the gel exclusion column under the same experimental condition as mentioned above. In the titration experiments with NaCl, 0.5% DDM was used and the ratio of trimer to monomer in the quenched condition was maintained for a few hours. The temperature dependency of the trimer dissociation of the NpHR sample in the absence of NaCl was measured using gel filtration chromatography as follows. First, the desalted 0.1% DDM−NpHR sample (20 μM) was incubated at 37−49 °C for 30 min to 3 h. Then, each sample was rapidly cooled in ice and water to quench the dissociation step, followed by measurement of the absorption spectra and gel filtration chromatography. A spectrophotometer (Model BioSpec-mini, Shimadzu, Kyoto, Japan) was used for the measurement of the visible absorption spectra. All experiments were performed in the dark.

Data Analysis. The timer fraction obtained from gel filtration chromatography as a function of the anion concentration was analyzed with the following equation: fraction = $[\text{anion}]^n/[(K_d^{app})^n + [\text{anion}]^n]$, where K_d^{app} and n are the apparent dissociation constant and Hill coefficient, respectively. To calculate the trimer dissociation rates in the presence of 0.1% DDM, the time courses of the trimer fraction were fitted to a two-exponential equation: fraction = $f\exp(-k_1t) + (1-f)\exp(-k_2t)$, where k_1 and k_2 are the dissociation rates and f is the dissociation component fraction with a dissociation rate of k_1. On the other hand, the thermal bleaching processes were well fitted to a single-exponential equation. The dissociation rates calculated in the temperature range of 37−49 °C were fitted to the Arrhenius equation: $K = A\exp(-E/RT)$, where A, E, R, and T are the frequency factor, activation energy (kilocalories per mole), gas constant (kilocalories per kelvin per mole), and temperature (kelvin), respectively. In the curve fitting, correlation coefficients were obtained.

RESULTS

Chloride Dependency of the Trimer Dissociation of NpHR. First, we examined the dependence of the chloride binding on the trimer dissociation of DDM-solubilized NpHR. Since we have found that the dissociation from a trimer to a monomer proceeded at a high temperature (for details, see below), the 0.5% DDM-solubilized NpHR samples were incubated at 40 °C with varying concentrations of chloride. After incubation for 3 h at 40 °C, samples were immediately cooled in ice and water to quench the trimer dissociation, followed size-exclusion chromatography at 25 °C. It was found that by the use

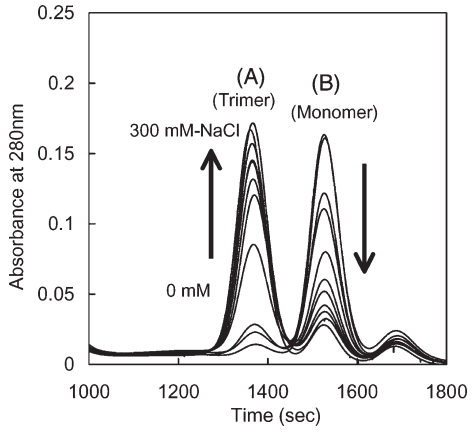

FIGURE 1: Gel filtration chromatogram of 0.5% DDM-solubilized NpHR after incubation at 40 °C for 3 h in the presence of 0−300 mM NaCl (pH 7). The samples were applied to a size-exclusion column previously equilibrated with 50 mM NaP_i (pH 7.0), 150 mM NaCl, and 0.1% DDM. The column was run at a flow rate of 500 μL/min, and eluting proteins were monitored at 280 nm. Peaks A and B represent the trimer and monomer of NpHR, respectively (see the text).

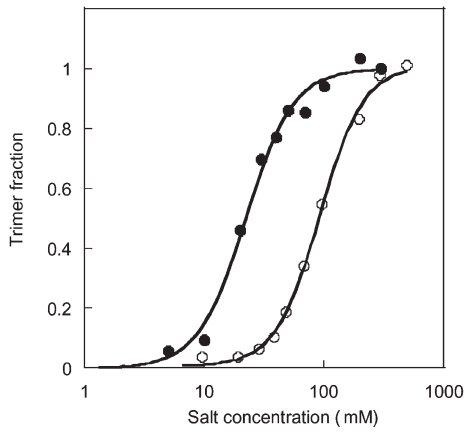

FIGURE 2: Proportion of the NpHR trimer as a function of anion concentration during the preincubation in 0.5% DDM at 40 °C for 3 h: chloride (●) and sulfate (○). The proportion of the NpHR trimer was calculated from the elution profile as shown in Figure 1. In the case of sulfate experiments, NpHR in the absence of chloride was used. Correlation coefficients for the curve fitting were > 0.995.

of this quenching method, the ratio of trimer to monomer was maintained for a few hours at 25 °C. Figure 1 shows the elution profiles in which two large peaks were observed at 1350 s (denoted by peak A) and 1500 s (peak B). As described in Materials and Methods, these peaks are attributed to the trimer and monomer of NpHR, respectively. It should be noted that there was no dimer peak in this detergent system. In the absence of chloride, peak A disappeared, indicating that the almost trimeric NpHRs dissociated to the monomer. In contrast, with increasing NaCl concentrations, the dissociation of the trimer was strongly prevented. These results indicate that the intermolecular interaction in the NpHR trimer was strengthened, and the dissociation of the trimer was prevented due probably to the Cl^- binding to the NpHR (see below and Discussion). The timer fraction as a function of the NaCl concentration obtained from Figure 1 showed a sigmoidal isotherm (Figure 2), suggesting that a cooperative salt binding or retaining of a trimer by NaCl addition. The apparent dissociation constant (K_d^{app}) for NaCl was 22 mM with a Hill coefficient of 2.2. Similarly, it was found that the trimer−monomer conversion of NpHR was controlled by SO_4^{2-} [K_d^{app} = 94 mM (Figure 2)]. It is known that SO_4^{2-} stabilizes the archaeal rhodopsins and, in the case of HR, does not bind to the Cl^- binding site at the Schiff base because of the lack of visual absorption changes (*17*). Similarly, the chloride and sulfate concentration dependency of the apparent rate constant of trimer dissociation was obtained from the change in the initial fraction (data not shown). The K_d^{app} for Cl^- was 13.4 mM with a Hill coefficient of 2.1 and for SO_4^{2-} was 59 mM with a Hill coefficient of 2.2. These results support a cooperative salt binding or retaining of a trimer by anion.

Kinetics of Thermal Dissociation and Bleaching in the Absence of Chloride. The kinetics of thermal dissociation of the NpHR trimer to the monomer with 0.1% DDM was measured in the absence of chloride. The DDM-solubilized NpHR solution with a final concentration of 20 μM was preincubated at 40 °C. After the predetermined incubation time, the sample was taken out and immediately cooled to quench the dissociation states, followed by application to the gel filtration column. Results are shown in Figure 3, revealing that with a decrease in trimer fraction, the monomer fraction increased cooperatively.

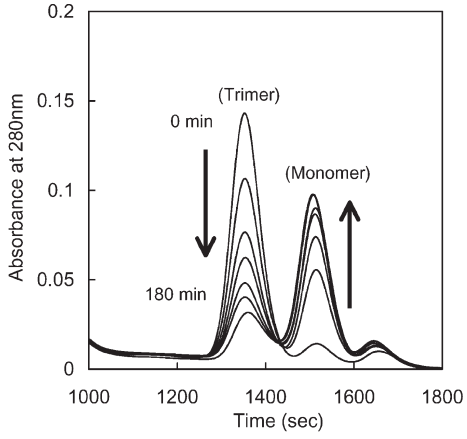

FIGURE 3: Gel filtration chromatogram of 0.1% DDM-solubilized NpHR after incubation at 40 °C for 0−180 min in the absence of Cl^-. The sample and experimental condition of the size-exclusion column were the same as those described in the legend of Figure 1.

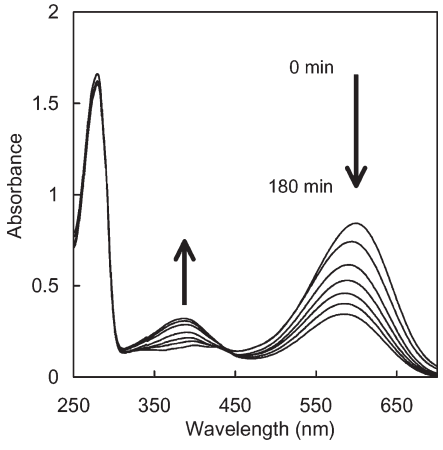

FIGURE 4: Visible absorption spectra of 0.1% DDM-solubilized NpHR after incubation at 40 °C for 0−180 min in the absence of Cl^-. The experimental condition was the same as that described in the legend of Figure 3.

In addition, we point out that the dimer fraction could not be detected. The visible absorption change of the corresponding time course was observed (Figure 4). Two apparently sequential

Table 1: Kinetic Parameters from the Analysis of Thermal Dissociation and Bleaching of the DDM−NpHR Complex[a]

	trimer dissociation rate (s^{-1})		
temp (°C)	fast component	slow component	bleaching rate (s^{-1})
37	1.1×10^{-4} (10)	4.7×10^{-5} (90)	5.5×10^{-5}
40	4.2×10^{-4} (29)	9.9×10^{-5} (71)	8.3×10^{-5}
43	7.0×10^{-4} (75)	6.8×10^{-5} (25)	1.4×10^{-4}
46	2.7×10^{-3} (67)	2.8×10^{-4} (33)	3.1×10^{-4}
49	3.5×10^{-3} (78)	4.1×10^{-4} (22)	6.2×10^{-4}

[a]The concentration of DDM was 0.1%. The trimer dissociation rate was monitored from the trimer peak from gel filtration chromatography. The bleaching rate was calculated from the degree of visible absorption at 580 nm. Values in parentheses represent the fraction of the fast and slow components.

effects are seen in Figure 4. The first is a minor blue shift of the absorption maximum from 600 nm at 25 °C to 580 nm at 40 °C, followed by slow bleaching with regard to the absorption maximum shift from 580 to 380 nm. This bleaching is explained by the hydrolysis reaction of the retinal Schiff base (*18*, *32*).

Similar experiments were performed for the temperature range from 37 to 49 °C. The time courses of the trimer fraction estimated by gel filtration chromatography are shown in Figure 5A, which shows that the rate of trimer dissociation increases with an increase in temperature. It is noted that the decrease in the trimer fraction could be fitted with a two-exponential equation. The rate constants estimated are listed in Table 1. As described above, the bleaching occurred simultaneously, and then the time coursed of that at varying temperatures are plotted in Figure 5B. Interestingly, the bleaching is well expressed in a single-exponential equation, and the bleaching rate matches approximately with the slow component of the trimer dissociation (Table 1).

Figure 6 shows the Arrhenius plots for the slow and fast rate constants of trimer dissociation and bleaching of the chloride-free NpHR. The dissociation rate of the fast component was ~1 order of magnitude faster than that of bleaching, implying the presence of the trimer−monomer conversion process before bleaching (as shown in Figure 7, the fast component corresponds to the solubilization process of the NpHR trimer). From the slopes of this Arrhenius plot, the activation energies for the fast and slow dissociation process were estimated to be 57.8 and 35.3 kcal/mol, respectively. On the other hand, the latter activation energy was close to the value obtained from the bleaching experiment, 40.5 kcal/mol.

The effect of the DDM concentration (0.1−0.5%) on the rates of both trimer dissociation and bleaching in the absence of chloride at 40 °C is shown in Figure 7. The fast component of the trimer dissociation rate was influenced by the DDM concentration, while the slow component of the dissociation and the bleaching rates were scarcely influenced by the detergent concentration. These results support the idea that the trimer association of the DDM−NpHR complex depends on the concentration of the nonionic detergent and the bleaching of the NpHR molecule after dissociation from the trimer to the monomer is independent of the concentration of the nonionic detergent.

DISCUSSION

Stabilization of Trimer Structure by Chloride Binding to the Second Binding Site. In this study, we found that NpHR

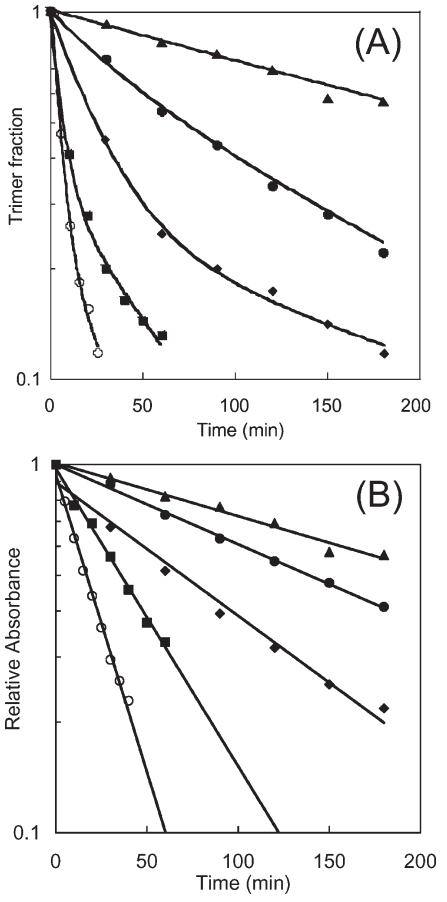

FIGURE 5: Time course of trimer dissociation (A) and bleaching (B) of the DDM−NpHR complex at (▲) 37, (●) 40, (◆) 43, (■) 46, and (○) 49 °C. Trimer dissociation was calculated from the trimer fraction peak of the gel filtration chromatogram, and bleaching was calculated from the maximum absorbance at ~580 nm. Correlation coefficients for the curve fitting were > 0.99.

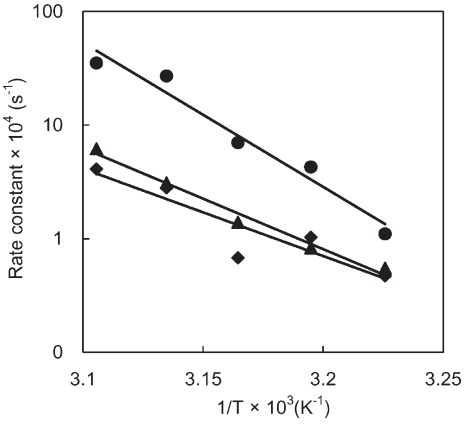

FIGURE 6: Arrhenius plots for the fast (●) and slow (◆) dissociation rates of the DDM−NpHR complex. The rate constant of the bleaching process (▲) was also plotted. Correlation coefficients for the curve fitting (fast, slow, and bleach) were 0.981, 0.91, and 0.991, respectively.

solubilized with DDM shows thermal dissociation from the trimer to the monomer in the absence of chloride. A sigmoidal isotherm obtained from the trimer fractions as a function of chloride concentration (Figure 2) showed a large apparent dissociation constant (K_d^{app} = 22 mM) compared with the K_d of chloride binding in the vicinity of the retinal Schiff base, 1−5 mM (Hill coefficient of 1.0) (*3*, *9*, *17*). Similarly, it was found

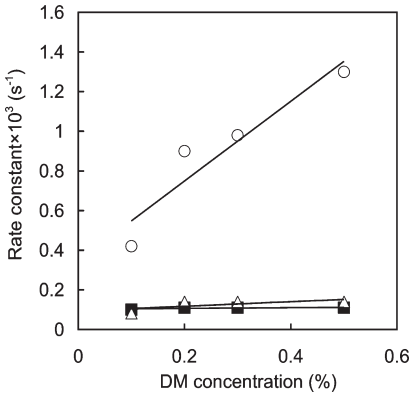

FIGURE 7: DDM concentration dependency of kinetic parameters, fast (○) and slow (■) dissociation and bleaching (△). Preincubation of the sample solution for calculation of these parameters was performed at 40 °C.

that the trimer−monomer conversion of NpHR was controlled by SO_4^{2-} [K_d^{app} = 94 mM (Figure 2)]. These results suggest that there is an anion binding site other than that next to the Schiff base of NpHR, to which Cl^- binds more strongly than SO_4^{2-}. Some researchers have also proposed the existence of the second anion-binding site. Lanyi and co-workers (*33*) first proposed the two binding sites of anions in the *salinarum* HR (HsHR); one (site II) is the site for the anion to be transported, and the other (site I) is the site for retaining the structure. With respect to NpHR, a weaker predicted Cl^- binding site on the extracellular (EC) side than that near the Schiff base has been proposed, with K_d values of 5−15 mM (*4*, *19*, *20*) that are close to our result estimated from the structural stability of the trimer (K_d^{app} = 22 mM). In addition, Mevorat-Kaplan et al. have reported that the hydrolysis reaction of the retinal Schiff base by heating is prevented when Cl^- binds to the site on the EC side (*18*). Similar privation of the bleaching was observed with the addition of not only NaCl but also Na_2SO_4 in this study (data not shown), supporting the binding of a SO_4^{2-} with the putative second binding site. A recent study of the high-resolution crystal structure of HsHR (T203V mutant) showed the second Cl^- binding site identified around Q105 and the two arginines, R103 and R24, on the EC side (*34*). However, in the case of NpHR, no corresponding residues are conserved in the same region. A crystal structure of bacteriorhodopsin (BR) under acidic conditions also showed the SO_4^{2-} binding on the surface of the EC side with a Hill coefficient of ~2 (*35*). The Hill coefficient values of 2.2 and 2.4 (for Cl^- and SO_4^{2-}, respectively) calculated from Figure 2 strongly suggest the cooperative anion binding ascribed to the intermolecular interaction among the NpHRs in the trimer. It was proposed that in an acidic solution of *pharaonis* phoborhodopsin (SR II), Cl^- may bind around Arg72 and Asp193 (*36*−*38*). The Cl^- binding occurs when Asp193 located at the EC surface is protonated. Considering these facts, we may infer that archaeal rhodopsins are capable of binding anions on the EC or CP surface under some conditions such as a lack or disappearance of the negative charge, and this binding contributes to the preservation of tertiary and quaternary structure. It is necessary to analyze the crystal structure of NpHR to identify the second chloride-binding site at the intermolecular surface.

Kinetic Consideration of Trimer Dissociation and Bleaching in the Absence of Chloride. Figure 8 shows a schematic drawing of the thermal trimer dissociation and bleaching of chloride-free NpHR in the dark. As described above,

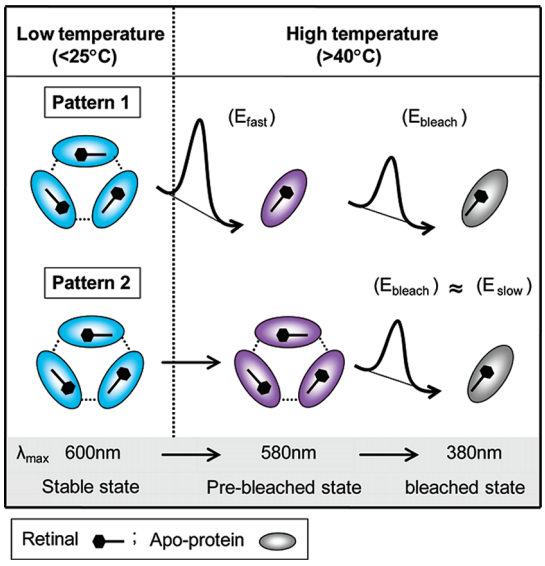

FIGURE 8: Schematic drawing for the dissociation and bleaching process of anion-free NpHR in the DDM detergent system. At low temperatures, anion-free NpHR with a λ_{max} of 600 nm (stable state) retains the trimer structure, which can be strengthened by specific anion binding. At high temperatures, the λ_{max} of NpHR shifts to ~580 nm (prebleached state) and the trimer structure dissociates to the monomer via two patterns (patterns 1 and 2), followed by the bleached state with a λ_{max} of 380 nm. E_{fast}, E_{slow}, and E_{bleach} are the activation energies for fast dissociation, slow dissociation, and bleaching, respectively. Values of those energies were 57.8 kcal/mol (E_{fast}), 35.3 kcal/mol (E_{slow}), and 40.5 kcal/mol (E_{bleach}), respectively.

NpHR in the presence of chloride has a high stability and retains the trimeric structure even under the high-temperature condition (> 40 °C). Contrary to this, intermolecular interaction in the NpHR trimer is weakened by release of the chloride, yielding dissociation to the monomer at high temperatures. As shown in Figure 5A, the trimer dissociation process in the absence of chloride has two components with fast and slow rate constants. The rate constant for the fast dissociation component was 1 order of magnitude larger than that for bleaching at high temperatures (> 40 °C). The activation energy for fast dissociation was higher by ~17 kcal/mol than that of bleaching (Figure 6). In addition, the λ_{max} of the NpHR solution at high temperatures was blue-shifted from 600 to 580 nm before the large blue shift to 380 nm by bleaching (Figure 4). These results suggest that after the NpHR trimer is dissociated by fast components, the NpHR molecule keeps a monomeric state with a λ_{max} of 580 nm for a while and then the monomer is bleached slowly ("pattern 1" of Figure 8).

The rate constant for fast dissociation was also strongly dependent on the detergent concentration as shown in Figure 7. Conversely, the bleaching rate was almost independent of it. This result also supports the idea that the bleaching process is independent of the dissociation process by the fast component. Interestingly, dissociation via the slow component proceeded at almost the same speed as that by bleaching, and the activation energy of 35.3 kcal/mol for the dissociation was also close in value to that for bleaching (Table 1 and Figure 6). The dependency of the slow dissociation component on the detergent concentration was scarcely observed as well as that of bleaching (Figure 7). The simplest model anticipated from these results is that in which bleaching and dissociation of the slow component occur cooperatively as shown in pattern 2 in Figure 8, although whether the slow dissociation component induces a bleaching

phenomenon or otherwise remains unresolved. One possibility of the presence of two patterns in the prebleached state is heterogeneity in the trimer population, corresponding to bound lipids or fatty acids. In our previous paper (*23*), mass spectroscopy of NpHR obtained from the *E. coli* expression system gave a sharp single peak at m/z 32276 that corresponds to one molecule of NpHR. The error between the observed and theoretical mass of His-tagged NpHR (32145) was 131, suggesting no bound lipids and fatty acids under our experimental condition. On the other hand, it has been reported that palmitate present in growth media remains bound to *H. salinarum* halorhodopsin (HsHR) during detergent purification with cholate and octyl glucoside washes, is present in samples used for crystallography, and is crystallographically resolved in a 1:1 complex with each monomer in the center of the halorhodopsin trimer on the extracellular face of the protein (*16*, *34*). On the other hand, NpHR was obtained from a cell-free system, which has no bound fatty acids, could be assembled into a homotrimer judging from the visual CD exciton band, and has a native photocycle as well as that obtained from *E. coli* cells, suggesting that individual NpHR needs no fatty acids for self-assembly. Further study of this is necessary. In summary, it is noted that the thermal bleaching is proceeded by a single component when the NpHR trimer is dissociated into monomer even through the different prebleached states as shown in Figure 8.

The tendency of the NpHR molecules to be bleached via a single component was not changed even though the fraction of each dissociation component had been changed (Table 1). These results suggest that the stability of the chloride-free NpHR in the dark is hardly affected by changes in the quaternary structure. If this assumption is correct, then we can conclude that the structural change by bleaching induces slow dissociation.

On the other hand, some studies have demonstrated that the formation of the trimer has an important role for retaining the thermal stability of NpHR and BR, especially in the light-irradiated state. In the case of BR, when the trimeric structure has been dissociated with an increase in temperature to >60 °C or solubilization by a nonionic detergent, BR under light irradiation is destabilized and finally leads to photobleaching (*28*, *39*, *40*). In addition, monomerization of BR and NpHR enhances the photobleaching by the hydroxylamine reaction under continuous illumination, implying that the intermolecular interaction between neighboring NpHR molecules in the trimer prevents the penetration of the hydroxylamine molecules into the internal region of the protein (*23*). A more recent study also revealed that a specific amino acid residue located in the transmembrane helix of NpHR is essential to stabilization of the trimeric helix−helix interaction. In addition, continuous light irradiation to the NpHR monomer induced different isometizations of retinal compared with the trimer (manuscript in preparation). From these studies, it is assumed that the oligomeric structure of archaeal rhodopsins may have a role in preventing the destabilization of the protein caused by the conformational changes in the photoexcited state, leading to the efficient ion pumping activity under the trimeric space. For example, the susceptibility to photons of one HR molecule might be dependent on whether the neighboring molecule is activated. Further study of this is necessary.

In conclusion, the homotrimer state of NpHR solubilized with DDM could be maintained in the both presence and absence of chloride at room temperature in the dark. However, the trimer−monomer conversion was accelerated in the absence of chloride when the temperature was above 40 °C, suggesting that the interface of the chloride-free NpHR trimer has a thermally sensitive structure compared with the chloride-bound form. Under this condition, the trimer dissociation rate corresponding to the fast component depended on both chloride and DDM concentration. These results suggest the presence of a secondary chloride-binding site at the CP or EC surface region that affects the intermolecular interaction in the trimeric NpHR molecules, and its anion selectivity is lower than that of the chloride-binding site at the Schiff base.

REFERENCES

1. Lanyi, J. K. (1990) Halorhodopsin, a light-driven electrogenic chloride-transport system. *Physiol. Rev. 70*, 319–330.
2. Matsuno-Yagi, A., and Mukohata, Y. (1980) ATP synthesis linked to light-dependent proton uptake in a red mutant strain of *Halobacterium* lacking bacteriorhodopsin. *Arch. Biochem. Biophys. 199*, 297–303.
3. Váró, G., Brown, L. S., Sasaki, J., Kandori, H., Maeda, A., Needleman, R., and Lanyi, J. K. (1995) Light-driven chloride ion transport by halorhodopsin from *Natronobacterium pharaonis*. 1. The photochemical cycle. *Biochemistry 34*, 14490–14499.
4. Váró, G., Needleman, R., and Lanyi, J. K. (1995) Light-driven chloride ion transport by halorhodopsin from *Natronobacterium pharaonis*. 2. Chloride release and uptake, protein conformation change, and thermodynamics. *Biochemistry 34*, 14500–14507.
5. Duschl, A., Lanyi, J. K., and Zimányi, L. (1990) Properties and photochemistry of a halorhodopsin from the haloalkalophile, *Natronobacterium pharaonis*. *J. Biol. Chem. 265*, 1261–1267.
6. Shimono, K., Iwamoto, M., Sumi, M., and Kamo, N. (1997) Functional expression of *pharaonis* phoborhodopsin in *Escherichia coli*. *FEBS Lett. 420*, 54–56.
7. Hohenfeld, I. P., Wegener, A. A., and Engelhard, M. (1999) Purification of histidine tagged bacteriorhodopsin, *pharaonis* halorhodopsin and *pharaonis* sensory rhodopsin II functionally expressed in *Escherichia coli*. *FEBS Lett. 442*, 198–202.
8. Sato, M., Kanamori, T., Kamo, N., Demura, M., and Nitta, K. (2002) Stopped-flow analysis on anion binding to blue-form halorhodopsin from *Natronobacterium pharaonis*: Comparison with the anion-uptake process during the photocycle. *Biochemistry 41*, 2452–2458.
9. Sato, M., Kubo, M., Aizawa, T., Kamo, N., Kikukawa, T., Nitta, K., and Demura, M. (2005) Role of putative anion-binding sites in cytoplasmic and extracellular channels of *Natronomonas pharaonis* halorhodopsin. *Biochemistry 44*, 4775–4784.
10. Hasegawa, C., Kikukawa, T., Miyauchi, S., Seki, A., Sudo, Y., Kubo, M., Demura, M., and Kamo, N. (2007) Interaction of the Halobacterial Transducer to a Halorhodopsin Mutant Engineered so as to Bind the Transducer: Cl^- Circulation within the Extracellular Channel. *Photochem. Photobiol. 83*, 293–302.
11. Sato, M., Kikukawa, T., Araiso, T., Okita, H., Shimono, K., Kamo, N., Demura, M., and Nitta, K. (2003) Roles of Ser130 and Thr126 in Chloride Binding and Photocycle of pharaonis Halorhodopsin. *J. Biochem. 134*, 151–158.
12. Sato, M., Kikukawa, T., Araiso, T., Okita, H., Shimono, K., Kamo, N., Demura, M., and Nitta, K. (2003) Ser-130 of *Natronobacterium pharaonis* Halorhodopsin Is Important for the Chloride Binding. *Biophys. Chem. 104*, 209–216.
13. Shibata, M., Muneda, N., Sasaki, T., Shimono, K., Kamo, N., Demura, M., and Kandori, H. (2005) Hydrogen-Bonding Alterations of the Protonated Schiff Base and Water Molecule in the Chloride Pump of *Natronobacterium pharaonis*. *Biochemistry 44*, 12279–12286.
14. Inoue, K., Kubo, M., Demura, M., Kamo, N., and Terazima, M. (2009) Reaction dynamics of halorhodopsin studied by time-resolved diffusion method. *Biophys. J. 96*, 3724–3734.
15. Kubo, M., Kikukawa, T., Miyauchi, S., Seki, A., Kamiya, M., Aizawa, T., Kawano, K., Kamo, N., and Demura, M. (2009) Role of Arg123 in light-driven anion pump mechanisms of *pharaonis* halorhodopsin. *Photochem. Photobiol. 85*, 547–555.
16. Kolbe, M., Besir, H., Essen, L. O., and Oesterhelt, D. (2000) Structure of the light-driven chloride pump halorhodopsin at 1.8 Å resolution. *Science 288*, 1390–1396.
17. Scharf, B., and Engelhard, M. (1994) Blue halorhodopsin from *Natronobacterium pharaonis*: Wavelength regulation by anions. *Biochemistry 33*, 6387–6393.
18. Mevorat-Kaplan, K., Brumfeld, V., Engelhard, M., and Sheves, M. (2006) The protonated Schiff base of halorhodopsin from *Natronobacterium*

pharaonis is hydrolyzed at elevated temperatures. *Photochem. Photobiol. 82*, 1414–1421.
19. Okuno, D., Asaumi, M., and Muneyuki, E. (2003) Chloride concentration dependency of the electrogenic activity of halorhodopsin. *Biochemistry 38*, 5422–5429.
20. Kalaidzidis, I. V., and Kalaidzidis, Y. L. (2003) Occupancy of two primary chloride-binding sites in *Natronobacterium pharaonis* halorhodopsin is a necessary condition for active anion transport. *Biochemistry* (*Moscow, Russ. Fed.*) *68*, 354–358.
21. Persike, N., Pfeiffer, M., Guckenberger, R., Radmacher, M., and Fritz, M. (2001) Direct observation of different surface structures on high-resolution images of native halorhodopsin. *J. Mol. Biol. 310*, 773–780.
22. Havelka, W. A., Henderson, R., Heymann, J. A. W., and Oesterhelt, D. (1993) Projection Structure of Halorhodopsin from *Halobacterium halobium* at 6 Å Resolution Obtained by Electron Cryo-microscopy. *J. Mol. Biol. 234*, 837–846.
23. Sasaki, T., Kubo, M., Kikukawa, T., Kamiya, M., Aizawa, T., Kawano, K., Kamo, N., and Demura, M. (2009) Halorhodopsin from *Natronomonas pharaonis* forms a trimer even in the presence of a detergent, dodectyl-β-D-maltoside. *Photochem. Photobiol. 85*, 130–136.
24. Karnaukhova, E., Vasileiou, C., Wang, A., Berova, N., Nakanishi, K., and Borhan, B. (2006) Circular dichroism of heterochromophoric and partially regenerated purple membrane: Search for exciton coupling. *Chirality 18*, 72–83.
25. Hasselbacher, C. A., Spudich, J. L., and Dewey, T. G. (1988) Circular dichroism of halorhodopsin: Comparison with bacteriorhodopsin and sensory rhodopsin. *Biochemistry 27*, 2540–2546.
26. Dencher, N. A., and Heyn, M. P. (1982) Preparation and properties of monomeric bacteriorhodopsin. *Methods Enzymol. 88*, 5–10.
27. Duschl, A., McCloskey, M. A., and Lanyi, J. K. (1988) Functional reconstitution of halorhodopsin. Properties of halorhodopsin-containing proteoliposomes. *J. Biol. Chem. 263*, 17016–17022.
28. Sasaki, T., Sonoyama, M., Demura, M., and Mitaku, S. (2005) Photobleaching of bacteriorhodopsin solubilized with Triton X-100. *Photochem. Photobiol. 81*, 1131–1137.
29. Zhang, F., Wang, L.-P., Brauner, M., Liewald, J. F., Kay, K., Natalie, W., Wood, P. G., Bamberg, E., Nagel, G., Gottschalk, A., and Deisseroth, K. (2007) Multimodal fast optical interrogation of neural circuitry. *Nature 446*, 633–639.
30. Seki, A., Miyauchi, S., Hayashi, S., Kikukawa, T., Kubo, M., Demura, M., Ganapathy, V., and Kamo, N. (2007) Heterologous expression of pharaonis halorhodopsin in *Xenopus laevis* oocytes and electrophysiological characterization of its light-driven Cl^- pump activity. *Biophys. J. 92*, 2559–2569.
31. Zhang, N., and Li, L. (2004) Effects of common surfactants on protein digestion and MALDI MS analysis of the digested peptides using two-layer sample preparation. *Rapid Commun. Mass Spectrom. 18*, 889–896.
32. Kubo, M., Sato, M., Aizawa, T., Kojima, C., Kamo, N., Mizuguchi, M., Kawano, K., and Demura, M. (2005) Dissociation and bleaching of chloride-free *pharaonis* halorhodopsin by octyl-β-glucoside. *Biochemistry 44*, 12923–12931.
33. Lanyi, J. K., Duschl, A., Váro, G., and Zimányi, L. (1990) Anion binding to the chloride pump, halorhodopsin, and its implications for the transport mechanism. *FEBS Lett. 265*, 1–6.
34. Gmelin, W., Zeth, K., Efremov, R., Heberle, J., Tittor, J., and Oesterhelt, D. (2007) The crystal structure of the L1 intermediate of halorhodopsin at 1.9 angstroms resolution. *Photochem. Photobiol. 83*, 369–377.
35. Okumura, H., Murakami, M., and Kouyama, T. (2005) Crystal structures of acid blue and alkaline purple forms of bacteriorhodopsin. *J. Mol. Biol. 351*, 481–495.
36. Iwamoto, M., Furutani, Y., Sudo, Y., Shimono, K., Kandori, H., and Kamo, N. (2002) Role of Asp193 in chromophore-protein interaction of *pharaonis* phoborhodopsin (sensory rhodopsin II). *Biophys. J. 83*, 1130–1135.
37. Iwamoto, M., Hasegawa, C., Sudo, Y., Shimono, K., Araiso, T., and Kamo, N. (2004) Proton release and uptake of *pharaonis* phoborhodopsin (sensory rhodopsin II) reconstituted into phospholipids. *Biochemistry 43*, 3195–3203.
38. Ikeura, Y., Shimono, K., Iwamoto, M., Sudo, Y., and Kamo, N. (2003) Arg-72 of *pharaonis* phoborhodopsin (sensory rhodopsin II) is important for the maintenance of the protein structure in the solubilized states. *Photochem. Photobiol. 77*, 96–100.
39. Yokoyama, Y., Sonoyama, M., and Mitaku, S. (2004) Inhomogeneous stability of bacteriorhodopsin in purple membrane against photobleaching at high temperature. *Proteins 54*, 442–454.
40. Mukai, Y., Kamo, N., and Mitaku, S. (1999) Light-induced denaturation of bacteriorhodopsin solubilized by octyl-β-glucoside. *Protein Eng. 12*, 755–759.